

# DoseCHECK™ & PerFRACTION™

On the Accuracy of the  
SNC Dose Calculator Algorithm

# Introduction

Sun Nuclear Corporation (SNC) patient QA products PerFRACTION™ and DoseCHECK™ utilize an advanced dose calculation engine that is new and unique in the radiation therapy market.

Whereas the intended purpose of the two products is different - PerFRACTION uses the SNC Dose Calculator (SDC) for pre-treatment QA (Fraction 0™) and in vivo QA (Fraction n™) while DoseCHECK uses the SDC to produce an entire dose volume to check against that from the Treatment Planning System (TPS) - both products pass the same required inputs to the SDC

and receive a full 3D dose volume in return. As with the introduction of any new radiotherapy dose calculation engine, one of the first questions that comes to the responsible clinical physicist's mind is, "How accurate is the dose calculation?" This white paper will answer that question and, in doing so, establish a baseline accuracy for the SDC.

## Dose Calculator Algorithm in Brief

Before describing the methods and results of this accuracy study, it is useful to briefly describe how the dose calculation engine works.

A more thorough description is available in the appendix for the interested reader. The SDC is a collapsed-cone convolution/superposition (C/S) algorithm<sup>1,2</sup> developed at The Johns Hopkins University.<sup>3,4</sup> The algorithm shares some of the same general themes of other C/S algorithms on the market, such as the same core steps involved in the calculation, namely:

1. Fluence Calculation (radiation transport within the accelerator head)
2. TERMA Calculation (radiation transport from the accelerator to the patient)
3. Superposition (radiation transport within the patient).

However the algorithm is quite unique in that it offers several advantages through its patent-protected<sup>5</sup> graphical processor unit (GPU) acceleration technology. Most notable among these advantages is the inverse

ray trace performed for the TERMA calculation and the inverse dose deposition during the superposition step, both of which are calculated in the GPU to take advantage of the massively parallel nature of these computational processes. Further, it is these performance gains that make other advantages possible that have heretofore not been possible due to computational limitations, such as:

- True dual-source model, each with their own spectrum and radial intensity definition (step 1)
- Explicit modeling of MLC parameters (step 1)
- Precise ray-tracing across boundaries while accounting for multiple material types and spectral changes during the TERMA computation (step 2)
- Kernel tilting, kernel hardening, and cumulative-cumulative kernel approach (step 3).

These are highlights of the algorithm; further details can be found in the appendix.

# Methods

At the highest level, this study involved four different comparisons of results from the SDC (version 1.0.1), including:

1. Ion chamber measurements
2. ArcCHECK™ measurements
3. ArcCHECK Planned Dose Perturbation (ACPDP) reconstructed dose
4. Treatment Planning System dose volume.

All studies and analyses were conducted at The H. Lee Moffitt Cancer Center, by Saeed Ahmed and Vladimir Feyselman. Details regarding the systems and instruments used for study are contained in Table 1.

Table 1: System/Instrument Details

System/Instrument	Type/Version Used
Treatment Planning System	Pinnacle <sup>3</sup> (version 9.8)
Delivery System and Beam Energy	Varian TrueBeam™ (version 2.0), Millennium 120 MLC, 6 MV
Case Types Studied	Anal, Head & Neck, Abdomen, and Lung
Ion Chamber	PTW 0.125 cm <sup>3</sup> Model TN31010
Homogenous Phantom	CIRS Plastic Water® Phantom
Anthropomorphic Phantom	CIRS IMRT Thorax Phantom
3D Measurement Phantom	Sun Nuclear ArcCHECK (software version 6.6.2)
3D Phantom Dose Reconstruction	Sun Nuclear 3DVH™ (version 3.2.0) ACPDP

The four Case Types are from the AAPM TG-244 Report library of test plans.<sup>6</sup> Treatment plans were generated in Pinnacle for all four cases using a 6 MV, 10 FFF, and 15 MV beam (Varian TrueBeam). For three of the four cases (Anal, Head & Neck, Abdomen), QA plans were calculated into the Plastic Water (PW) phantom. For the final case (Lung), a QA plan was generated on the Thorax phantom. The four cases were delivered to their respective phantoms with the ion chamber inserted accordingly, and also to the ArcCHECK device. Results were then compared. This methods workflow is depicted below in Figure 1.

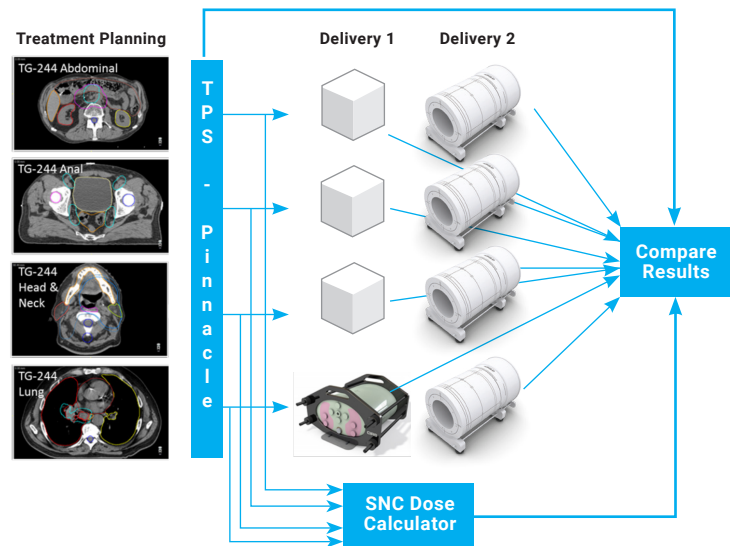


Figure 1. Workflow followed for this study.

# Results and Discussion

## SDC vs. Ion Chamber

The calculated point doses are compared to the ion chamber measurements in Table 2. The primary TPS data are also presented for completeness. The SDC exhibits 0.2% average deviation from the ion chamber, well within the 1.5% recommended by TG-244 for the primary TPS in the high dose low gradient area.

TG-244 Patient/Test	Phantom	Point	Plan	6 MV		10 FFF		15 MV	
				SDC - IC (%)	Pinn. - IC (%)	SDC - IC (%)	Pinn. - IC (%)	SDC - IC (%)	Pinn. - IC (%)
ABDOMEN	PW Cube	Cube center	VMAT	0.6	1.0	0.3	0.6	0.8	0.8
			IMRT	0.1	-0.3	-0.1	-0.3	-0.05	-0.1
Head & Neck	PW Cube	Cube center	VMAT	-0.9	1.0	0.4	1.0	-0.3	0.6
			WFIMRT	-0.4	1.2	0.9	1.1	-0.8	0.6
ANAL	PW Cube	Cube center	VMAT	-2.0	1.4	-0.6	-1.6	-0.3	0.9
			WFIMRT	-1.1	2.0	0.01	1.0	-1.3	1.4
LUNG	CIRS Thorax	Target	VMAT	2.6	3.1	1.1	0.9	4.0	1.4
			WFIMRT	1.9	2.1	1.8	1.4	2.8	1.2
		"Mediastinum"	VMAT	1.3	2.5	-0.6	-2.0	-1.5	-2.8
			WFIMRT	0.3	0.8	-1.0	-4.0	-1.2	-5.4
<b>Average</b>				<b>0.2</b>	<b>1.5</b>	<b>0.2</b>	<b>-0.2</b>	<b>0.2</b>	<b>-0.1</b>
<b>St. Dev.</b>				<b>1.4</b>	<b>1.0</b>	<b>0.9</b>	<b>1.8</b>	<b>1.8</b>	<b>2.2</b>

Table 2. Relative local percent difference between calculations (the SDC and Pinnacle) and ion chamber measurements.

## SDC vs. ArcCHECK

According to criteria in the upcoming AAPM TG-218 report, the tolerance limit (treatable but further evaluation may be warranted) should be set at 95% of points passing the 3% Global/2mm/10% gamma analysis, with the action limit set at 90% (requires additional analysis and may need corrective action). The SDC produces agreement with ArcCHECK above the tolerance limit in all the studied cases but one (Table 3). The  $\gamma$  passing rate is 93.5% for the wide-field IMRT Anal plan, still above the action limit of 90%. This is one of the most challenging plan classes computationally, combining large bifurcating targets (requires very accurate dose modeling under the MLC) with the wide-field technique that imposes rather stringent accuracy requirement on the leaf penumbra model in the TPS.

TG-244 Patient/Test	Plan	6 MV		10 FFF		15 MV	
		SDC Pass rate (%)	Median $\Delta D$ (SDC-AC, %)	SDC Pass rate (%)	Median $\Delta D$ (SDC-AC, %)	SDC Pass rate (%)	Median $\Delta D$ (SDC-AC, %)
ABDOMEN	VMAT	100	-1.3	100	0.7	100	0.9
	IMRT	99.1	-1.3	98.0	1.3	99.0	0.6
Head&Neck	VMAT	99.7	-2.2	98.6	2.9	99.9	1.0
	WFIMRT	98.6	-2.5	96.7	2.0	98.8	0.03
ANAL	VMAT	99.2	-3.4	98.2	1.9	99.5	0.4
	WFIMRT	93.5	-3.4	97.3	1.5	98.2	0.04
LUNG	VMAT	99.8	-0.5	96.0	3.4	98.3	2.3
	WFIMRT	99.1	-1.5	94.5	1.9	97.6	0.8
<b>Average</b>		<b>98.6</b>	<b>-2.0</b>	<b>97.4</b>	<b>2.0</b>	<b>98.9</b>	<b>0.8</b>
<b>St. Dev.</b>		<b>2.1</b>	<b>1.0</b>	<b>1.7</b>	<b>0.9</b>	<b>0.9</b>	<b>0.7</b>

Table 3. Gamma analysis (3% Global, 2mm) passing rates and median dose-difference (Global normalization) across all points: SDC vs. direct AC measurements.

## SDC vs. MGDR

In the next step, the agreement between ArcCHECK PDP, a measurement-guided dose reconstruction on the patient dataset for which accuracy has been previously established<sup>7,8</sup> and the SDC follows the same trend as the direct comparison on the homogeneous phantom (Table 4). The only test case falling below the 95% agreement level is again the wide field IMRT Anal plan, for the same reasons as discussed above. The remaining ACPDP 3D doses for both VMAT and IMRT plans agree with the SDC for 96.4% of the points or better.

TG-244 Patient/Test	Plan	6 MV		10 FFF		15 MV	
		SDC Pass rate (%)	Median ΔD (SDC-AC, %)	SDC Pass rate (%)	Median ΔD (SDC-AC, %)	SDC Pass rate (%)	Median ΔD (SDC-AC, %)
ABDOMEN	VMAT	99.9	-0.5	98.9	-0.3	99.7	0.29
	IMRT	99.9	-0.3	99.6	1.0	100	0.26
Head&Neck	VMAT	98.2	-1.0	96.3	2.6	99.1	0.6
	WFIMRT	98.9	0.1	95.9	2.7	98.7	0.2
ANAL	VMAT	96.4	-3.0	99.0	1.5	99.5	-1.53
	WFIMRT	91.8	-3.2	98.7	1.2	97.0	-2.18
LUNG	VMAT	98.1	0.5	90.4	4.3	90.9	2.6
	WFIMRT	98.6	0.7	94.5	3.1	95.8	1.7
	<b>Average</b>	<b>97.7</b>	<b>-0.8</b>	<b>96.7</b>	<b>2.0</b>	<b>97.6</b>	<b>0.2</b>
	<b>St. Dev.</b>	<b>2.6</b>	<b>1.5</b>	<b>3.1</b>	<b>1.4</b>	<b>3.1</b>	<b>1.6</b>

Table 4. Gamma analysis (3% Global, 2mm) passing rates and median dose-difference (Global normalization) across all points: SDC vs. 3D measurement guided dose reconstruction on the patient dataset (ACPDP).

## SDC vs. Pinnacle

Finally, the doses generated by Pinnacle and SDC are quantitatively compared in Table 5. Gamma analysis passing rates are well above 95% for all cases.

TG-244 Patient/Test	Plan	6 MV		10 FFF		15 MV	
		SDC Pass rate (%)	Median ΔD (SDC-TPS, %)	SDC Pass rate (%)	Median ΔD (SDC-TPS, %)	SDC Pass rate (%)	Median ΔD (SDC-TPS, %)
ABDOMEN	VMAT	99.9	-0.02	99.3	0.4	99.8	1.07
	IMRT	100.0	0.5	99.9	0.9	100	1.43
Head&Neck	VMAT	99.8	-0.8	98.7	2.3	97.5	1.5
	WFIMRT	99.8	-0.1	97.7	3.2	96.3	2.0
ANAL	VMAT	99.9	-0.5	98.7	2.0	99.1	1.05
	WFIMRT	99.8	0.0	98.8	2.8	99.7	1.35
LUNG	VMAT	100.0	1.3	98.9	3.8	93.4	4.9
	WFIMRT	99.8	1.8	98.6	3.4	96.3	3.7
	<b>Average</b>	<b>99.9</b>	<b>0.3</b>	<b>98.8</b>	<b>2.4</b>	<b>97.8</b>	<b>2.1</b>
	<b>St. Dev.</b>	<b>0.1</b>	<b>0.9</b>	<b>0.6</b>	<b>1.2</b>	<b>2.3</b>	<b>1.4</b>

Table 5. Gamma analysis (3% Global, 2mm) passing rates with different dose-error thresholds and normalizations, and median dose-differences: SDC vs. Pinnacle.

# Conclusions

Comparisons between the SDC and direct measurements (ion chamber and diode array), as well as with semi-empirical volumetric dose reconstruction (ACDPD), indicate that the SDC performs at the accuracy level expected from a primary TPS, on rather challenging cases. This is based on the TG-244 expectation of the mean dose disagreement with the ion chamber not exceeding 1.5% and the emerging routine patient QA standard of 95% of the dose distribution passing the  $\gamma$ (3% Global, 2mm, 10%) analysis.

# References

1. Mackie TR, Scrimger JW, Battista JJ. A convolution method of calculating dose for 15-MV x-rays. *Med Phys.* 1985 Mar-Apr; 12(2):188-96.
2. Ahnesjo A. Collapsed cone convolution of radiant energy for photon dose calculation in heterogeneous media. *Med Phys.* 1989 Jul-Aug; 16(4):577-92.
3. Jacques R, Taylor R, Wong J, McNutt T. Towards real-time radiation therapy: GPU accelerated superposition/convolution. *Comput Methods Programs Biomed.* 2010 Jun; 98(3):285-92.
4. Jacques R, Wong J, Taylor R, McNutt T. Real-time dose computation: GPU-accelerated source modeling and superposition/convolution. *Med Phys.* 2011 Jan; 38(1):294-305.
5. McNutt, Todd, and Robert Jacques. Real-time dose computation for radiation therapy using graphics processing unit acceleration of the convolution/superposition dose computation method. The Johns Hopkins University, assignee. Patent US 8,325,878 B2. 04 Issued: 04 Dec. 2012 (Priority Date: 08 May 2008).
6. Smilowitz JB, Das IJ, Feygelman V et al. AAPM Medical Physics Practice Guideline 5.a.: Commissioning and QA of Treatment Planning Dose Calculations – Megavoltage Photon and Electron Beams. *J Appl Clin Med Phys.* 2015; 16 (5):14-34.
7. Nelms BE, Opp D, Robinson J, Wolf TK, Zhang G, Moros E, Feygelman V. VMAT QA: measurement-guided 4D dose reconstruction on a patient. *Med Phys.* 2012 Jul; 39(7):4228-38.
8. Opp D, Nelms BE, Zhang G, Stevens C, Feygelman V. Validation of measurement-guided 3D VMAT dose reconstruction on a heterogeneous anthropomorphic phantom. *J Appl Clin Med Phys.* 2013 Jul 8; 14(4):4154.

# Appendix

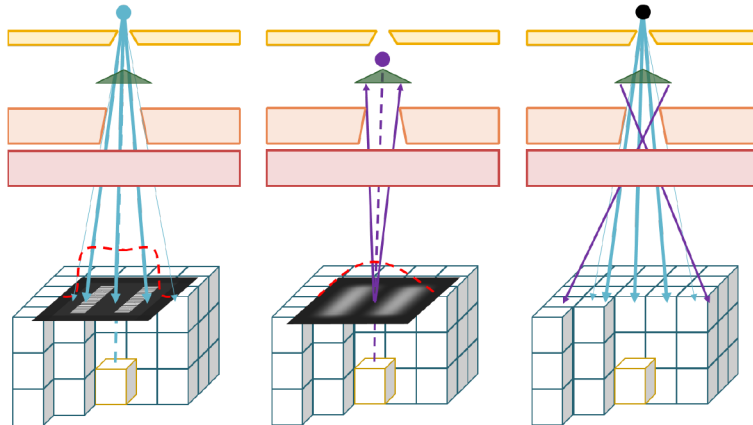
The dose calculator evaluated in this study was the SNC Dose Calculator (SDC) used in the PerFRACTION™ and DoseCHECK™ products from Sun Nuclear Corporation (Melbourne, FL). This dose calculator employs a collapsed-cone convolution/superposition (C/S) style dose calculation. The dose calculation consists of three steps:

1. Fluence Calculation (radiation transport within the accelerator head)
2. TERMA Calculation (radiation transport from the accelerator to the patient)
3. Superposition (radiation transport within the patient).

Before these steps begin, a relative electron density volume is created using the CT image volume, CT-to-electron density data, and DICOM structure density override information (if applicable). This relative electron density volume is used in the three main steps detailed below.

# Fluence Calculation

The fluence calculation is responsible for simulating radiation transport within the linear accelerator treatment head. The inputs to the fluence calculation are a model of the linear accelerator head and the DICOM RT Plan. The outputs are fluence distributions for both the primary and extrafocal (i.e. scatter or secondary) sources. This dual-source model is depicted in Appendix Figure 1.



Appendix Figure 1. Dual source fluence model

## Technical Highlights

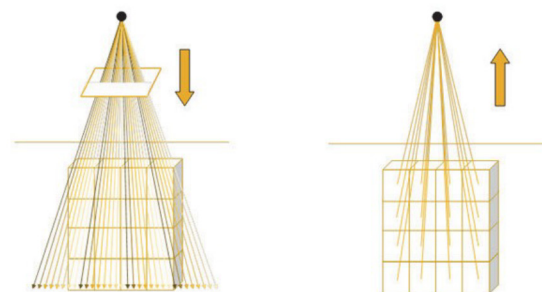
- Separate sources used to model primary, extra focal (scatter), and electron contamination radiation, each possessing their own weighting factor relative to the other components.
- The primary and extrafocal sources have their own spectrum and arbitrary radial intensity profile. The electron contamination source has its own spectrum.
- Accounts for transport through jaws and MLC completely, including aspects such as MLC tongue-and-groove thickness and MLC leaf end curvature.

# TERMA Calculation

The TERMA (or Total Energy Released per unit MAss) calculation describes radiation transport from the time it leaves the accelerator head to the time it first interacts within the patient. As the name indicates, TERMA describes the distribution of energy released within the patient.

## Technical Highlights

- Inverse ray-tracing done to maximize GPU benefits (Appendix Figure 2)
- Exact radiological pathlength tracing (versus fixed step size)
- Pathlengths across 9 different material types are tracked during the ray trace process. These 9 values are subsequently combined with a 16-component energy spectrum to accurately characterize attenuation.
- Calculated every two degrees for VMAT



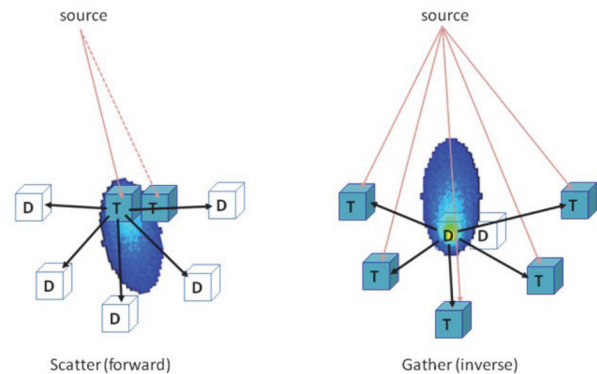
Appendix Figure 2. Forward versus inverse TERMA calculation.

# Superposition Calculation

Superposition accounts for radiation transport within the patient. When megavoltage x-rays interact in tissue, their energy is not deposited all at once; instead, the first interaction begins a shower of secondary photons, electrons, and positrons, which spread their energy throughout the patient volume. This energy spread is accounted for using dose spread arrays, also known as superposition kernels.

## Technical Highlights

- Inverse superposition done to maximize GPU benefits (Appendix Figure 3)
- Collapsed Cone approximation with 90 anisotropic directions chosen to maximize forward-focused contributions to dose.
- Cumulative Cumulative Kernel (CCK) approach<sup>1</sup> used to minimize voxelization effects
- Kernel tilting and kernel hardening<sup>2,3</sup> over two energy bins used
- High resolution (1 mm, 1 degree) kernel
- Radiological Path Length indexing used to account for inhomogeneities
- Exact radiological pathlength tracing (versus fixed step size)
- Dose computed on a grid with 2.5 mm spacing (all dimensions)
- Calculation performed every five degrees for VMAT



Appendix Figure 3. Forward versus inverse Superposition operation.

# Appendix References

1. Lu W, Olivera GH, Chen ML, Reckwerdt PJ, Mackie TR. Accurate convolution/superposition for multi-resolution dose calculation using cumulative tabulated kernels. *Phys Med Biol.* 2005 Feb 21; 50(4):655-80.
2. Papanikolaou N, Mackie TR, Meger-Wells C, Gehring M, Reckwerdt P. Investigation of the convolution method for polyenergetic spectra. *Med Phys.* 1993 Sep-Oct; 20(5):1327-36.
3. Liu HH, Mackie TR, McCullough EC. Correcting kernel tilting and hardening in convolution superposition dose calculations for clinical divergent and polychromatic photon beams. *Med Phys.* 1997 Nov; 24(11):1729-41.